Fabrication of auxetic foam sheets for sports applications

ALLEN, Tom <http://orcid.org/0000-0003-4910-9149>, HEWAGE, Trishan, NEWTON-MANN, Chloe, WANG, Weizhuo, DUNCAN, Oliver and ALDERSON, Andrew <http://orcid.org/0000-0002-6281-2624>

Published version

ALLEN, Tom, HEWAGE, Trishan, NEWTON-MANN, Chloe, WANG, Weizhuo, DUNCAN, Oliver and ALDERSON, Andrew (2017). Fabrication of auxetic foam sheets for sports applications. physica status solidi (b), 254 (12), p. 1700596.

Fabrication of auxetic foam sheets for sports applications

Abstract

Auxetic materials have a negative Poisson's ratio, which can enhance other properties. Greater indentation resistance and energy absorption, as well as synclastic curvature, could lend auxetic materials well to protective sports equipment and clothing. Sheets of foam often form padding within protective equipment, but producing large homogenous auxetic foam samples is challenging. The aim of this work was to investigate techniques to fabricate large thin sheets of auxetic foam, to facilitate future production and testing of prototype sports equipment utilising this material. A mould was developed to fabricate sheets of auxetic foam - with planar dimensions measuring 350 x 350 mm – using the thermo-mechanical process. The mould utilised through-thickness rods to control lateral compression of foam. Sheets of auxetic foam measuring 10 x 350 x 350 mm were fabricated and characterised. Each sheet was cut into nine segments, with density measurements used to determine how evenly the foam had been compressed during fabrication. Specimens cut from corner and centre segments were subject to quasi-static extension up to 30% to obtain stress vs. strain relationships, with Digital Image Correlation used to determine Poisson's ratio. Specimens cut from the corner tended to have a marginally higher density, lower stiffness and more consistent negative Poisson's ratio compared to those from the centre, indicating some inconsistency in the conversion process. Future work could look to improve fabrication techniques for large thin homogenous sheets of auxetic foam.

Keywords: Protection; digital image correlation; equipment; clothing; material

1. Introduction

Auxetic materials have a negative Poisson's ratio (NPR), they expand laterally when stretched and contract laterally when compressed [1-4]. Auxetic behaviour can influence other properties - increasing indentation resistance and shear modulus (in isotropic materials) [5-7], while reducing bulk modulus and increasing energy absorption [5, 6] and providing synclastic curvature - which could lend these materials well to sports equipment [4-6] and clothing. Sports brands are demonstrating interest in auxetic structures via patents [11, 12] and their associated products. Vibration damping [13-15] and crushing performance [13] of auxetic foam is superior to its conventional parent foam. Under impact, auxetic foam tends to deform less (resisting "bottoming out") [16] and reduce peak forces [17-19], in comparison to its conventional counterpart, indicating it may be well suited to sports products. Allen et al. [20] highlighted potential for auxetic foam in snowsport safety devices.

Lakes [1] was the first to fabricate auxetic foam, converting conventional, thermoplastic open-cell foam with a thermo-mechanical process. Typically, foam is compressed tri-axially to around a third of its volume in a mould, which buckles cell ribs [1]. The mould and foams are heated to soften the foam and encourage permanent uptake of compression, then left to cool and stiffen to give a contorted re-entrant cell structure [1, 14, 17, 21, 22]. Expansion of contorted, re-entrant cells under tension, or contraction under compression, results in an NPR [1, 6, 23, 24].

Since Lakes' proposed thermo-mechanical fabrication method [1], multiple heating cycles [25], an annealing stage [7, 22] and hand stretching [25] have been added. Olive oil has also been applied to lubricate the internal surface of moulds and reduce surface creasing [26]. Annealing, hand stretching and mould lubrication are not always used, and successful fabrications are possible without them [27, 28]. Alternatives to the thermo-mechanical fabrication process [1] include using a solvent (i.e. Acetone [29] or pressurised CO_2 [30]) as a softening agent. Approaches can be mixed, and both acetone [19] and CO_2 [30] have been used in combination with heat.

Despite a wealth of research into auxetic foam, producing large samples with consistent properties remains challenging, it is hard to apply even compression throughout and achieve a re-entrant cell structure at the centre [9, 10, 21, 22, 31-33]. Options to increase homogeneity when converting large samples of foam include using i) a mould with moveable walls which can be assembled around the foam to apply compression [31, 32], ii) a multi-stage compression process with an intermediate compression ratio [22], iii) a vacuum bag to apply compression [33], and iv) rods passed through the thickness of sheets of foam to control planar compression [10, 20, 34].

Out of the suggested solutions to the challenge of fabricating large samples of auxetic foam, the only option that has been compared to a simple compression regime in a standard mould (i.e. without moving parts, an intermediate compression level or a vacuum bag) is passing rods through the foam [10, 34]. Rods can control lateral compression, highlighted by the fabrication of gradient sheets [34], but they also leave holes through the foam [10, 34]. Foam sheets fabricated with rods to control planar compression in tri-axially compressed conversions had comparable variability in density (when dissected [34]), Poisson's ratio and Young's modulus to sheets fabricated without rods [10, 34], suggesting they were neither beneficial nor detrimental. Comparisons between conversions with and without rods have only used limited dimensions (~350 x ~350 x 20 mm [34] and 150 x 150 x 30 mm [10]), although rods have been used to fabricate larger (~350 x ~350 x 70 mm) samples [20]). This work aims to fabricate large sheets of auxetic foam with a reduced thickness of 10 mm, to aid future work on the production and testing of prototype sports products utilising this material, such as padded clothing, footwear and protective equipment.

2. Methods

Open-cell polyurethane foam (R30RF, supplied by Custom Foams) was converted to auxetic foam, following multistage thermo-mechanical conversion methods outlined in recent work with the same material [20, 34]. A bespoke aluminium mould – utilising through-thickness rods to control lateral compression - was developed to fabricate large thin sheets of auxetic foam measuring 10 x 350 x 350 mm (Figure 1a). The level of compression applied during fabrication is defined by the Linear Compressions Ratio (LCR), corresponding to the ratio of the compressed dimension to the original dimension in each direction. A lower ratio equates to more compression, which is thought to produce a more contorted re-entrant cell structure and increase the magnitude of NPR [9, 17]. Unconverted foam sheets measured 14 x 500 x 500 mm and 17 x 583 x 583 mm, so the mould would impose LCRs of 0.6 and 0.7.

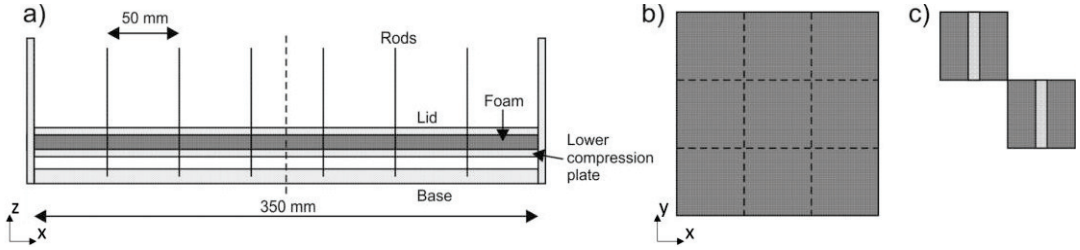

Fig. 1. Illustrations showing, a) cross-sectional view of closed mould with compressed foam and through-thickness rods, b) converted foam sheet including locations of nine segments and c) corner and centre segments including locations of tensile specimens.

A uniform grid of thirty-six holes (3.1 mm diameter, with 50 mm centre to centre spacing) was drilled through the mould's lid and lower compression plate, and into the base, to accommodate an equal number of silver steel rods (3.1 mm in diameter). An acrylic sheet (5 mm thick) containing a similar grid of holes with the required spacing served as a template for inserting the rods through the foam, prior to its insertion into the mould. The rods were located in corresponding holes in the mould, as the foam was positioned inside, to control lateral compression. The mould was then put in an oven (Carbolite PF60) for 25 minutes at 180 °C, after which the foam was removed and gently stretched by hand. The process was repeated once and followed by an annealing stage for 20 minutes at 100 °C, after which the foam was left to cool in the mould at room temperature.

The density of converted foam was calculated from measurements taken with a ruler and digital weighing scale (Mettler PE11), to determine how evenly it had been compressed. Samples were cut into nine segments (Figure 1b) and the density of each one was divided by the mean of all those from the sheet, to obtain a normalised value. A cuboidal specimen - measuring 10 x 20 x 117 mm - was cut from a corner and the centre segment from each sheet for tensile testing (Figure 1c). An unconverted foam specimen of the same dimensions was also tested. Testing was performed in a uniaxial test device (Hounsfield H10KS, Olsen) fitted with a 100 N load cell (Figure 2). The pneumatic clamps (HT400) were set 60 mm apart with a pressure of 138 kPa holding the specimen as it was stretched to 30% at

5 mm/min (0.0014 s^{-1}). Force and displacement were recorded, with engineering stress obtained from specimen dimensions.

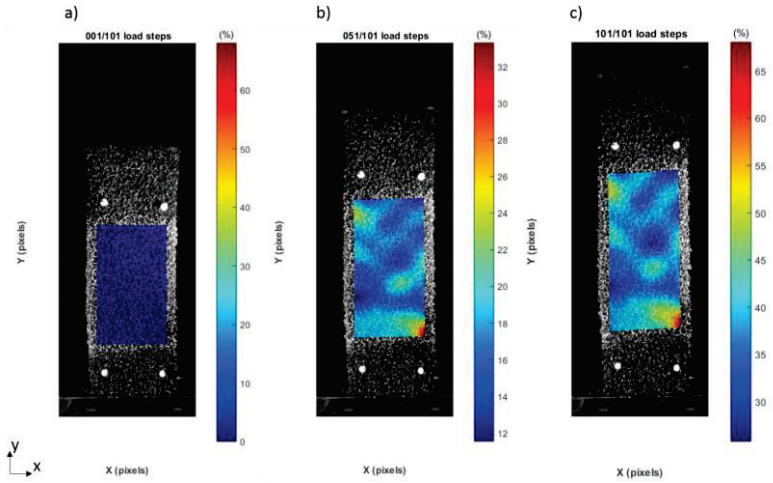

Fig. 2. Front surface of tensile specimen in testing device as viewed from the camera, showing speckle pattern for DIC and superimposed longitudinal strain, a) no extension, b) mid-test: averaged strain 16.8% finite / 15.5% infinitesimal and c) full extension: averaged strain 37% finite / 31.8% infinitesimal. Specimen corresponds to 0.7 through-thickness LCR with pins retained taken from the centre.

Optical Digital Image Correlation (DIC) [35] was used to obtain full field measurements of lateral strain, longitudinal strain and Poisson's ratio, only previously applied to micro-ct scans of in-situ tensile tests of auxetic foam [36]. Surfaces of specimens were painted with a silver marker pen to create a speckle pattern (Figure 2). A camera (Nikon D3200 with AF MICRO NIKKOR 60 mm 1:2.8 D lens, 6,016 x 4,000 pixels) positioned with its optical axis parallel to the face of the specimen was manually triggered to obtain approximately one hundred images throughout the trial. Specimens were tested four times with a different surface facing the camera for each trial. Manual analysis was performed digitally on the images in figure 2 - to obtain longitudinal engineering strain using the visible white pinheads and clamps - for comparison against the results obtained from DIC. Longitudinal strain was calculated using, i) the pin-to-pin distance and ii) the clamp-to-clamp distance.

The plan was to produce samples with LCRs of 0.6 and 0.7, but achieving these levels of lateral compression without creases and/or folds in converted sheets proved challenging and unfeasible with the proposed method. Following attempts to solve the problem, the lateral LCR was increased to 0.8, by trimming foam from unconverted sheets to reduce planar dimensions. Prior to conversion, trimmed sheets measured 14 x 438 x 438 mm for a through-thickness LCR of 0.7 and 17 x 438 x 438 mm for a through-thickness LCR of 0.6. The foam retained compression after the first heating phase, allowing it to be returned to the mould with ease, but there were holes in converted samples where rods had passed through, as reported by Duncan et al. [10, 34]. While rods may aid insertion of unconverted foam into the mould, it was unclear if they were required to retain lateral compression once the lid was secured. Two sheets of auxetic foam were fabricated for each through-thickness LCR, one with the rods retained when the mould was in the oven and the other with them removed, resulting in a total of four.

3. Results

Figure 3 illustrates normalised density of segments cut from converted sheets. Considering limitations in the accuracy of foam cutting and positioning rods and samples within the mould, combined with uncertainty in dimension measures and variation in unconverted foam (27-32 kg/m^3, as stated by supplier), densities were almost consistent between segments. Mean results in figure 3e do, however, indicate segments from the centre tended to have a marginally lower density.

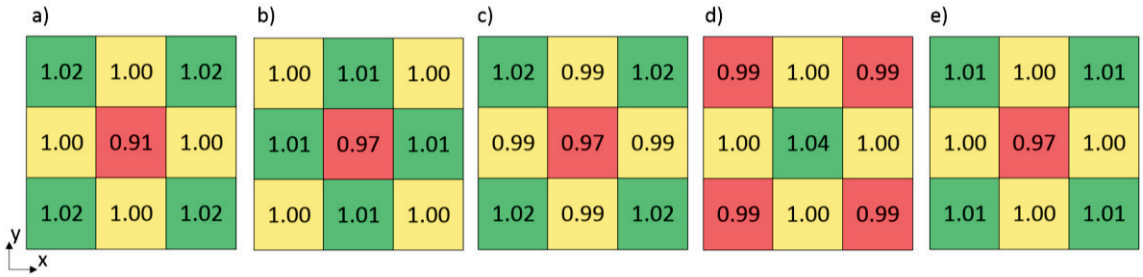

Fig. 3. Normalised density of segments, a) through-thickness LCR of 0.7, rods retained, b) through-thickness LCR of 0.7, rods removed, c) through-thickness LCR of 0.6, rods retained, d) through-thickness LCR of 0.6, rods removed and e) mean of all four sheets. Values for the corner and centre are the mean of four segments from corresponding positions. Green = highest, yellow = medium and red = lowest, for each sheet.

Figure 4 shows mean tensile engineering stress vs. strain relationships for the foam. The stress vs. strain relationship for the unconverted foam was similar to that reported by Duncan et al. [31]. Converted foam tended to exhibit lower stress for a given strain compared to its unconverted counterpart, particularly at higher levels of extension, indicating lower stiffness. Stress vs. strain relationships for foam taken from centre of the converted sheets tended to exhibit intermediate behaviour when compared to corner and unconverted specimens. Samples corresponding to foam conversions with rods retained during heating tended to have a lower stress for a given strain, although this was not always the case.

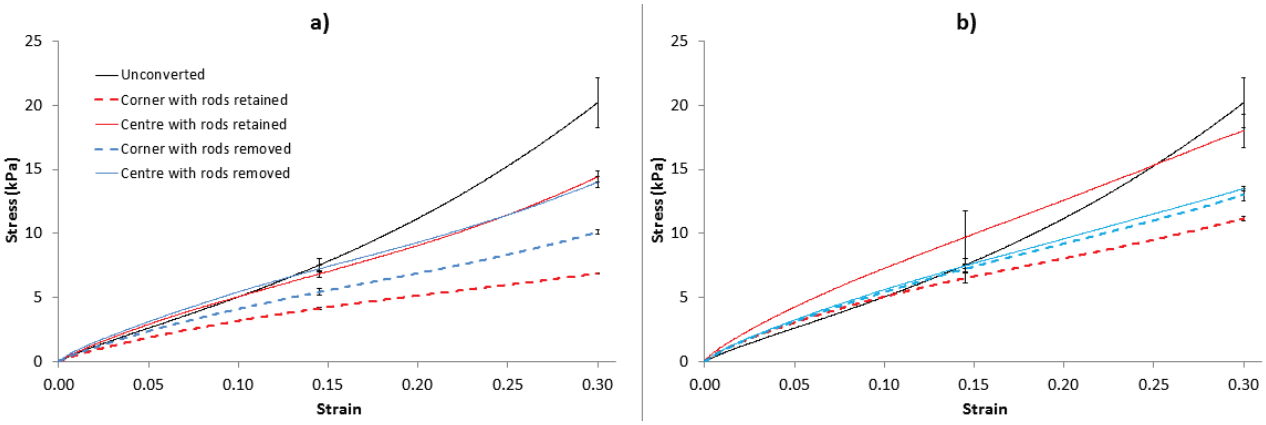

Fig. 4. Mean tensile stress vs. strain relationships for samples with lateral LCR of 0.8 and through-thickness LCR of, a) 0.7 and b) 0.6. Error bars represent one standard deviation either side.

Manual analysis of images from figure 2 for longitudinal engineering strain gave values of 15% for figure 2b (pin-to-pin and clamp-to-clamp) and 31% (pin-to-pin) and 30% (clamp-to-clamp) for figure 2c, as expected from applied extension and in broad agreement with DIC outputs indicating they are valid.

Figure 5 shows the front face (20 mm wide) of a tensile specimen – corner of the sheet with a through-thickness LCR of 0.7 - with superimposed DIC plots for longitudinal strain (a), lateral strain (b) and Poisson's ratio (c). The Poisson ratio plot in figure 5c indicates the foam was auxetic. Figure 5d shows Poisson's ratio vs. true longitudinal strain for the front face of this converted tensile specimen, as well as the unconverted foam. Unconverted foam exhibited a positive Poisson's ratio between 0.3 and 0.5, comparable with findings of Duncan et al. [34]. In contrast, converted foam had an NPR between -0.15 and -0.25.

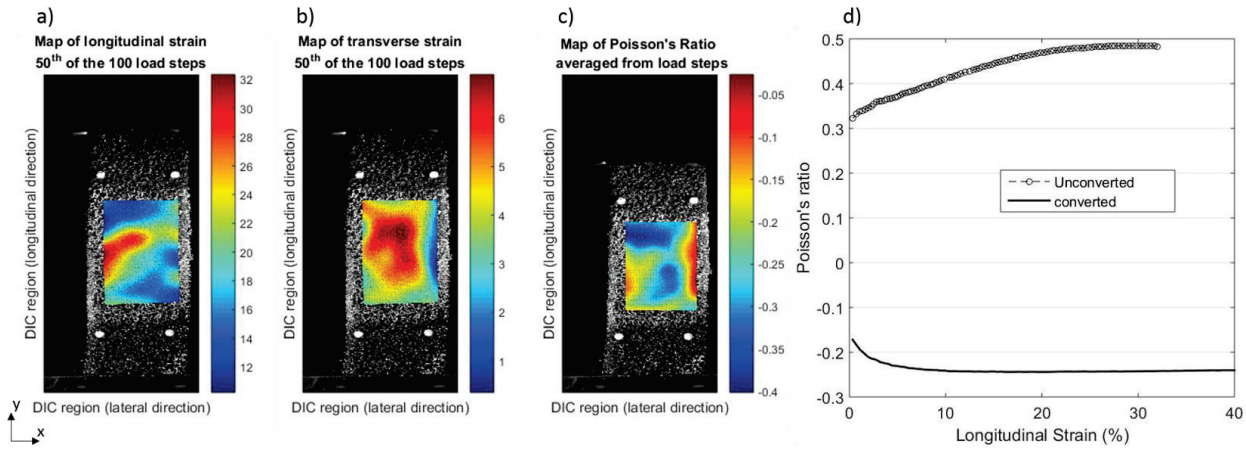

Fig. 5. Front surface of converted tensile specimen with superimposed, a) longitudinal strain mid test, b) lateral strain mid test, c) Poisson's ratio averaged from all load steps. d) Poisson's ratio vs. longitudinal strain for front face of converted and unconverted specimen. Converted specimen corresponds to 0.7 through-thickness LCR with rods retained taken from the corner.

Figure 6 shows Poisson's ratio vs. true longitudinal strain for all converted specimens. Converted foam exhibited auxetic behaviour, with Poisson's ratios tending to fall between 0 and -0.4. Some specimens did, however, exhibit positive Poisson's ratios just above zero (~0 to 0.15), indicating some inconsistency in the conversion process. Specimen from the corner of the sheets tended to exhibit greater magnitude of NPR than those from the centre, particularly for the front/back face, in agreement with the density results in figure 3 and the stress vs strain relationships in figure 4. The side faces (10 mm wide) of the specimens also tended to exhibit a greater magnitude of NPR (range ~-1 to -4) than the front/back faces (range ~1.5 to -2.5), as expected from the lower LCR though the thickness of the foam. Foam converted with rods retained during heating tended to exhibit greater magnitude of NPR, although this was not always the case.

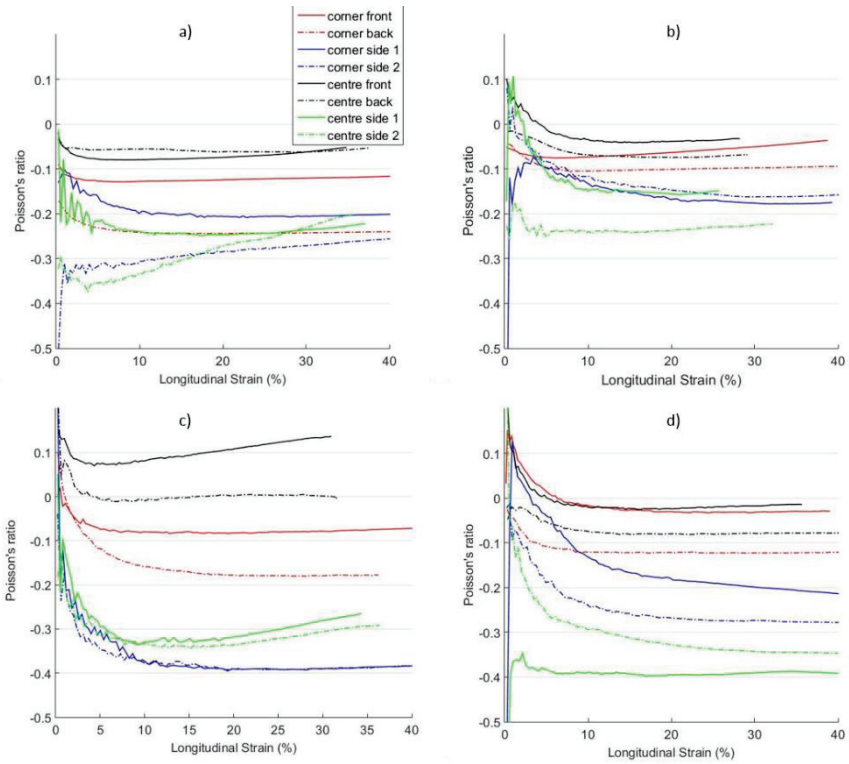

Fig. 6. Poisson's ratio vs. longitudinal strain for all faces of each tensile specimen with lateral LCR of 0.8 and through-thickness LCR of, a) 0.7 with rods retained, b) 0.7 with rods removed, c) 0.6 with rods retained and d) 0.6 with rods removed. Poisson's ratio of side face corresponds to lateral expansion through the thickness direction, which had a lower LCR.

4. Discussion

Large thin sheets of auxetic foam - measuring 10 x 350 x 350 mm - were fabricated with a modified thermo-mechanical process. Through-thickness rods appeared to assist insertion and compression of large thin sheets of unconverted foam within the mould. Using the method presented here, however, it was not possible to impose lateral compression ratios of 0.7 or smaller, without excessive creases and/or folds in converted samples. Trimming material to reduce planar dimensions of unconverted sheets aided fabrication, but reduced lateral compression during conversion appeared to result in anisotropic auxetic foam, as expected from previous work [25, 34]. Future work should look to develop the techniques to enable greater flexibility in, and control of, the fabrication process, to facilitate production of isotropic or anisotropic sheets of auxetic foam, as required for specific applications. Indentation theory [5-7] relies on isotropy, and further work should also characterise auxetic foams fabricated with anisotropic compression ratios in all three orthogonal planes. Greater magnitude of NPR can also be achieved with an anisotropic material than an isotropic material (which is limited to the range of -1 to 0.5) [3, 5, 22, 37, 38].

Characterisation of converted foam indicated sheets were not evenly compressed during fabrication. Foam from the corner of converted sheets tended to have marginally higher density, lower stiffness and more consistent NPR, indicating this region was compressed more than the centre. Tailoring the number, and placement, of through-thickness rods used to control lateral compression may help to produce homogenous sheets of auxetic foam. Using a lubricant to aid insertion of foam into the mould could further reduce flaws and heterogeneity [26] . The best approach, however, may be to combine through-thickness rods with the method proposed by Chan and Evans [22], where different sized moulds were used to increase foam compression with each heating cycle. An approach combining staged compression and fewer rods, with lower diameter, should limit the presence of through-thickness holes in converted foam. This study is limited to four conversions, and future work systematically comparing fabrication methods with more samples would be beneficial.

The results indicate that retaining through-thickness rods during heating results in more uniform and consistent conversions, with greater magnitude of NPR. The specific effect of retaining the through-thickness rods does, however, remain unclear due to the limited number of samples converted here. Future work could look more specifically into whether there is an advantage of retaining through-thickness rods across a greater number of samples, a range of imposed compression ratios and sheets of different size and thickness. Work of this nature would benefit from analysis of the cellular structure of the foam, as done in previous studies [9, 17, 20, 34]. Future work should also investigate different foams, of varying stiffness, to determine the most suitable candidates for sports applications.

5. Conclusion

Sheets of auxetic foam measuring 10 x 350 x 350 mm were fabricated, with the thermo-mechanical process, in a mould utilising through-thickness rods to control lateral compression. The lateral compression ratio was 0.8 and through-thickness compression ratios were 0.6 and 0.7, depending on the thickness of the unconverted foam. Converted foam was inhomogeneous, with marginally lower density at the centre of the sheets than the corners. Future work will look to produce large homogenous sheets of auxetic foam with higher-imposed compression, while fabricating and testing prototype sports products utilising this material.

Acknowledgements

We acknowledge Mr Mike Green for his technical assistance.

References

[1] R. Lakes, *Science* **1987**, *235*, 1038.
[2] K. W. Wojciechowski, *Molecular Physics* **1987**, *61*, 1247.
[3] T. C. Lim, *Auxetic Materials and Structures*, Springer, Singapore **2015**, p. 587.
[4] M. F. Ashby, L. J. Gibson, *Cellular solids: structure and properties*. Cambridge, UK: Press Syndicate of the University of Cambridge **1997**.
[5] K. E. Evans, A. Alderson, *Advanced Materials* **2000**, *12*, 617.
[6] K. K. Saxena, R. Das, E. P. Calius, *Advanced Engineering* Materials **2016**, *18*, 1847.
[7] N. Chan, K. E. Evans. *Journal of Cellular Plastics* **1998**, *34*, 231.
[8] M. Sanami, N. Ravirala, K. Alderson, A. Alderson, *Procedia Engineering* **2014**, *72*, 453.
[9] O. Duncan, L. Foster, T. Senior, A. Alderson, T. Allen. *Smart Mater. Struct.* **2016**, 25, 054014.
[10] O. Duncan, L. Foster, T. Senior, T. Allen, A. Alderson, *Procedia Engineering* **2016**, *147*, 384. http://doi.org/10.1016/j.proeng.2016.06.323
[11] T. M. Cross, K. W. Hoffer, D. P. Jones, P. B. Kirschner, E. Langvin, J. C. Meschter, Nike, Inc. **2015**. *Auxetic structures and footwear with soles having auxetic structures* US patent 20,150,245,685, 3 Sep 2015.
[12] A. Toronjo, **2013**. *Articles of apparel including auxetic materials*. US Patent Application 13/838,827, filed 15 March 2013.
[13] F. Scarpa, L. G. Ciffo, J. R. Yates, *Smart Mater. Struct.* **2003**, *13*, 49.
[14] F. Scarpa, P. Pastorino, A. Garelli, S. Patsias, M. Ruzzene, *Phys Status Solidi B* **2005**, *242*, 681.
[15] F. Scarpa, J. Giacomin, Y. Zhang, P. Pastorino. *Cellular Polymers* **2005**, *24*, 253.
[16] T. Allen, N. Martinello, D. Zampieri, T. Hewage, T. Senior, L. Foster, A. Alderson, *Procedia Engineering* **2015**, *112*, 104.
[17] T. Allen, J. Shepherd, T.A.M. Hewage,T. Senior, L. Foster, A. Alderson, *Phys Status Solidi B* **2015**, *252*, 1631.
[18] C. Ge, *Journal of Cellular Plastics* **2013**, *49*, 521. doi:10.1177/0021955X13503844.
[19] J. Lisiecki, T. Błazejewicz, S. Kłysz, G. Gmurczyk, P. Reymer, G. Mikułowski. *Phys Status Solidi B* **2013**, 250 (10): 1988–95. doi:10.1002/pssb.201384232.
[20] T. Allen, O. Duncan, L. Foster, T. Senior, D. Zampieri, V. Edeh, A. Alderson, In *Snow Sports Trauma and Safety* (Eds: I. Scher, R. Greenwald, N. Petrone), Springer, Cham **2017**, pp. 145-159.

[21] R. Critchley, I. Corni, J. A. Wharton, F.C. Walsh, R. J. Wood, K. R. Stokes, *Phys Status Solidi B* **2013**, *250*, 1963.
[22] N. Chan, K.E. Evans, *Journal of Materials Science* **1997**, *32*, 5945.
[23] J. N. Grima, R. Gatt, N. Ravirala, A. Alderson, K.E. Evans, *Materials Science and Engineering: A* **2006**, *423*, 214
[24] A. A. Pozniak, J. Smardzewski, K. W. Wojciechowski, *Smart Mater. Struct.* **2013**, *22*, 8.
[25] A. Alderson, K. L. Alderson, P. J. Davies, G. M. Smart, In *ASME 2005 International Mechanical Engineering Congress and Exposition,* American Society of Mechanical Engineers, **2005**, pp. 503-510.
[26] J.B. Choi & R.S. Lakes, *J Mater Sci* **1992**, 27: 4678. https://doi.org/10.1007/BF01166005
[27] Y. Li, C. Zeng, *Polymer* **2016**, *87*, 98. http://doi.org/10.1016/j.polymer.2016.01.076
[28] K. Boba, M. Bianchi, G. McCombe, R. Gatt, A. C. Griffin, R. M. Richardson, F. Scarpa, I. Hamerton, J. N. Grima. *ACS Appl. Mater. Interfaces* **2016**, *8*, 20319. http://doi.org/10.1021/acsami.6b02809
[29] J. N. Grima, D. Attard, R. Gatt, R. N. Cassar, *Adv. Eng. Mater.* **2009**, *11*, 533. doi:10.1002/adem.200800388.
[30] Y. Li, C. Zeng, *Advanced Materials* **2016**, *28*, 2822. http://doi.org/10.1002/adma.201505650
[31] A. Lowe, R. S. Lakes, *Cellular Polymers* **2000**, *19*, 157.
[32] M. A. Loureiro, R. S. Lakes, *Cellular Polymers* **1997**, *16*, 349.
[33] M. Bianchi, F. Scarpa, M. Banse, C. W. Smith, *Acta Materialia* **2011**, *59*, 686. http://doi.org/10.1016/j.actamat.2010.10.006
[34] O. Duncan, T. Allen, L. Foster, T. Senior, A. Alderson, *Acta Materialia* **2017**, 126, 426.
[35] E. M. C. Jones **2015** Matlab-based DIC code, Available via: https://uk.mathworks.com/matlabcentral/fileexchange/.
[36] F. Pierron, *The Journal of Strain Analysis for Engineering Design* **2010**, *45*, 233.
[37] B. D. Caddock, K. E. Evans, *J. Phys. D: Appl. Phys.* **1989**, *22*, 1877.
[38] K.E. Evans, B.D. Caddock, *J. Phys. D: Appl. Phys.* **1989**, *22*, 1883.